AN ABSTRACT OF THE THESIS OF

Changho Kwon for the degree of Master of Science in Electrical and Computer Engineering presented on August 22, 2012.

Title: Performance and Optimization of Pulsed UWB Localization with Large Number of Sources

Abstract approved:

____

Huaping Liu

Pulsed ultra-wideband (UWB) radio uses extremely short pulses to transmit information. Such pulses provide very fine timing information, which has led to technological advances in high-precision localization. This thesis focuses on techniques and experiments of Time-Difference-of-Arrival (TDOA) localization of a large number of simultaneous sources. First, common localization techniques such as Received Signal Strength (RSS), Angle of Arrival (AOA), Time of Arrival (TOA), and TDOA are reviewed. It is concluded that TDOA method is best suited for the target application – localization of a large number of targets/sources all required to have simple hardware/software. Then, an algorithm to select a subset of Gold codes from the complete set of a certain code length is developed for minimum mutual interference. This optimized subset of codes is used in simulation. Finally, an experiment is conducted in a warehouse. The goal is to detect and localize the desired transmitter with the 'intended' code from a total of 100 active targets. Two different scenarios are studied in the experiment; all transmitters are synchronized (Case 1) and all transmitters are asynchronous (Case 2). For both

cases, experimental results have shown that the codes optimized are effective for high-precision localization of a large number of simultaneous sources.

Performance and Optimization of Pulsed UWB Localization with Large Number of Sources

by

Changho Kwon

A THESIS

submitted to

Oregon State University

in partial fulfillment of
the requirements for the
degree of

Master of Science

Presented August 22, 2012
Commencement June 2013

Master of Science thesis of Changho Kwon presented on August 22, 2012

APPROVED:

Major Professor, representing Electrical and Computer Engineering

Director of the School of Electrical Engineering and Computer Science

Dean of the Graduate School

I understand that my thesis will become part of the permanent collection of Oregon State University libraries. My signature below authorizes release of my thesis to any reader upon request.

Changho Kwon, Author

ACKNOWLEDGEMENTS

First, thanks God. “I can do all this through him who gives me strength.” (Philippians 4:13)

I would like to acknowledge my advising professor Dr. Huaping Liu for his invaluable advice, excellent guidance and continuous encouragement throughout whole time in OSU. I would never able to complete my thesis without his help. I am also very thankful to his understanding and caring to my study and life, especially about a lot of kids! He has been like a mentor as a father of 4 kids.

Thanks also go to Dr. Hamdaoui, Dr. Wang, and Dr. Coop for their great efforts and significant amount of time to serve on my M.S. thesis committee.

I would like to thank Arash Abbasi, Stephen Redfield, Tianzhu Qiao, and Ruiqing Ye for many helps and useful discussion on the coursework and thesis. Especially, I am deeply indebted to Arash Abbasi and Stephen Redfield.

I also want to express my deepest gratitude to the government and Air Force of Republic of Korea for giving me the chance to study abroad and providing financial support. I will serve the ROKAF for good.

Finally, I would like to express my deepest love and appreciation to my love, Sunsook An, who is always cheering me up and trusts me. And love for my kids, Haneul, Hagyeong, and Hayeon Kwon. I confess that you are the most valuable treasure of my life. Without their constant encouragement, smile, and unconditional love, it would have been impossible to finish my graduate study successfully. I love you all.

TABLE OF CONTENTS

Page

TABLE OF CONTENTS (Continued)

Page

LIST OF FIGURES

LIST OF FIGURES (Continued)

LIST OF TABLES

DEDICATION

To my wife Sunny, for standing by me through the good times and bad times. I adore you and admire your personality.

Chapter 1 – Introduction

This chapter aims to provide a fundamental knowledge of Ultra-Wideband (UWB) wireless communication technology such as technological aspects, current regulations in the U.S, and military applications already or potentially existing in the world. One could realize the reason why UWB technology becomes attractive for accurate localization systems by understanding the characteristics of UWB provided in this chapter.

1.1 Overview of UWB

UWB signals have an extremely wide bandwidth with a weaker average power than that of conventional narrowband signals. More specifically, as shown in Figure 1.1, the absolute bandwidth refers to the difference between the upper frequency f_H of the -10 dB emission point and the lower frequency f_L of the -10 dB emission point.

$$B_w = f_H - f_L ,$$

which is also called -10 dB bandwidth. The fractional bandwidth is defined as

$$B_{fr} = \frac{B_w}{f_c} ,$$

where f_c is the center frequency and is given by

$$f_c = \frac{f_H + f_L}{2}.$$

UWB signals either have a bandwidth equal to or greater than 500 MHz regardless of the fractional bandwidth, or have a fractional bandwidth equal to or greater than 0.20 [1].

It is important to note that the allowed radiated power of a UWB system is not to exceed the FCC Part 15 Limit, the maximum transmit power for electrical equipment that is not designed to radiate. The regulations of UWB will be explained in Section 1.3.

Historically, UWB radar systems were primarily developed as a military device because they have the capability of ′see through′ obstacles and beneath ground surfaces. Recently, however, UWB technology has been applied for commercial electronics and communications.

UWB technology is different from conventional narrowband wireless transmission technology − instead of broadcasting on separate frequencies, UWB spreads signals across a very wide range of frequencies. The typical sinusoidal radio wave is replaced by trains of pulses [2].

The large bandwidth of UWB signals provides numerous advantages for localization, communications, and radar applications such as penetration through obstacles, accurate localization, high-speed data transmission, and low cost and low power transceiver designs. The penetration capability of a UWB signal comes from its large frequency spectrum including high-frequency components as well as low-frequency ones. The large spectrum also gives high time resolution which improves range estimation accuracy.

Pulsed UWB systems are specified by extremely short duration pulses (e.g., on the order of a nanosecond). A pulsed UWB system commonly transmits such short duration pulses with a low duty cycle. Such a scheme is called impulse radio (IR) UWB [3]. For localization systems, the main aim is to estimate position-related parameters of the IR UWB signal, such as time-of-arrival (TOA). This will be discussed in Chapter 2.

1.2 Shannon's Theory

The benefits and the potential of UWB perhaps can be best summarized by examining Shannon's capacity equation. This equation would be familiar to anyone who has studied communication or information theory. Shannon's capacity equation for Additive White Gaussian Noise (AWGN) channels is expressed as

$$C = B \log(1 + S/N),$$

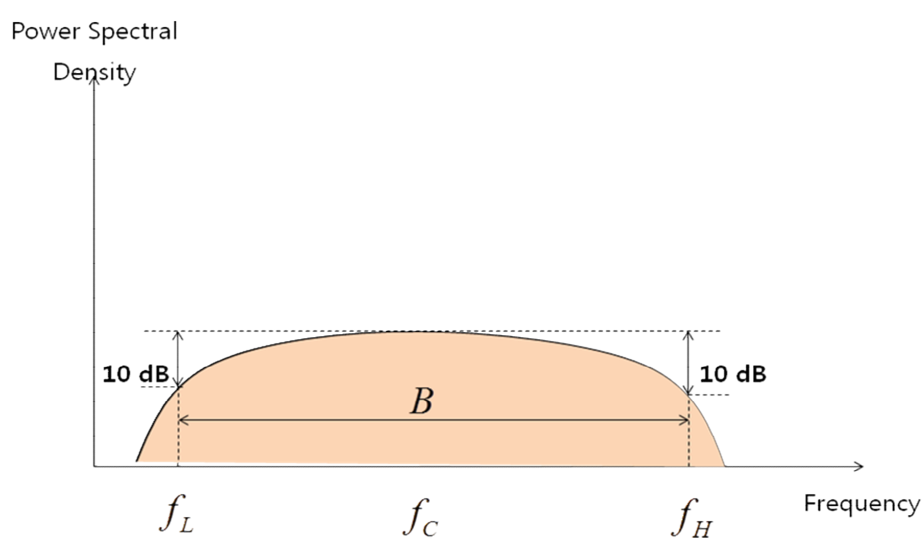

Figure 1.1: UWB signal bandwidth definition [1]

where C is the maximum channel capacity in bits per second, B is the channel bandwidth in hertz, S is the average received signal power in watts, and N is the average received noise power in watts.

This equation provides us with three ways to improve the channel capacity: increase bandwidth, increase signal power, or decrease noise. Commonly, the S/N ratio is known as the *signal-to-noise ratio* (SNR) of the channel. We can see that the channel capacity increases linearly with bandwidth B, but only logarithmically with signal power S. Consequently, UWB devices can have a much lower operating power than conventional narrowband communication systems.

The UWB channel has an adequate bandwidth and in fact can trade off some of the bandwidth for reduced signal power and interference from other sources. Thus, we can learn that UWB systems have a great potential for high capacity wireless communications from Shannon′s equation [2].

1.3 Regulatory

The UWB signals need to coexist with the existing systems with as little interference as possible because UWB signals occupy a very wide range of frequencies. Therefore, The Federal Communications Commission (FCC) has set a spectral mask to regulate UWB communications. UWB regulation sets upper bounds on the average power spectral density (PSD), which must not exceed -41.3 dBm/MHz over the frequency band from 3.1 GHz to 10.6 GHz, and is usually specified as a spectral mask described in Fig. 1.2 and Table 1.1. Note that these numbers are in terms of the Effective Isotropic Radiated Power (EIRP), the amount of power required for an ideal isotropic antenna to emit peak power equivalent to the given application's antenna in its direction of maximum gain.

The FCC Part 15 regulations permit the operation of categories of radio frequency devices without the need for a license or frequency coordination. The regulations also attempt to decrease the probability of unlicensed devices causing harmful interference to other users of the radio spectrum. The U.S. FCC issued a First Report and Order for UWB technology and authorized the commercial deployment of UWB technology, subject to technological and operational constraints [4].

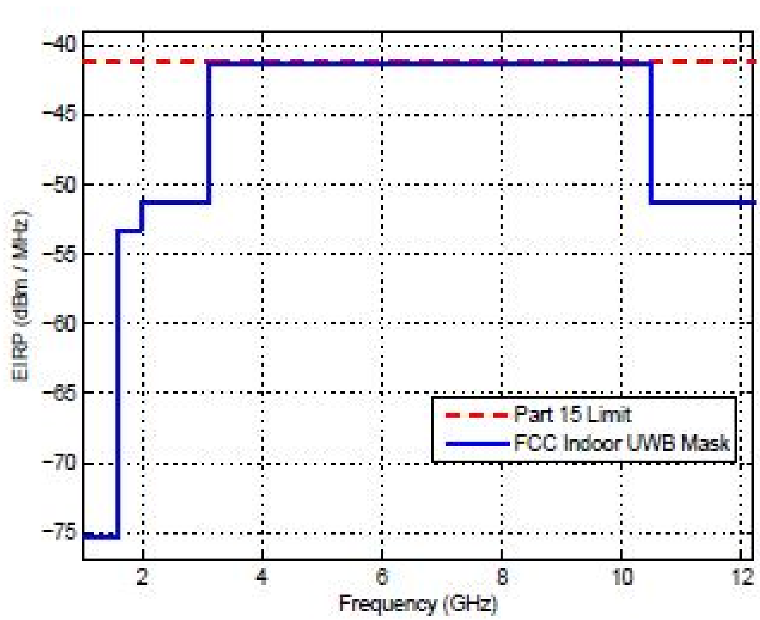

Figure 1.2: FCC UWB spectral mask versus Part 15 Limit [1]

Frequency (MHz)	EIRP (dBm)
960 - 1610	-75.3
1610 - 1990	-53.3
1990 - 3100	-51.3
3100 - 10600	-41.3
Above 10600	-51.3

Table 1.1: FCC Indoor UWB EIRP Mask [1]

1.4 Military Applications of UWB Technology

As stated in Section 1.1, UWB technology was initially developed in the military for radar and communications applications due to its unique properties such as material penetration capability and immunity to interference. UWB technology had been restricted to military areas under classified programs from the 1960s to the 1990s [2] [3].

Radar is considered as one of the main applications of UWB technology. The fine positioning characteristic of short-duration UWB pulses allows them to offer high-resolution radar for military applications. UWB signals also can penetrate various obstacles due to the ultra wide frequency spectrum. This unique characteristic makes UWB ground-penetrating radar (GPR) a critical asset for rescue and recovery units for detecting survivors buried under such as collapsed buildings in disaster situations. UWB radar could offer practical advantages such as tracking or surveillance systems with a low probability of detection by the spectral characteristics of the signal as long as security is maintained. U.S. Army, for example, adopted UWB systems to track trainees engaged in a mock village comprised of a number of multi-floor, cinderblock buildings [5].

UWB radio for covert military communications has been an attractive technology due to the low transmission power of UWB pulses which are extremely difficult to intercept or detect. Therefore, secure military information is protected from unauthorized parties. Also, UWB devices can be manufactured in small sizes at a lower cost than conventional communication systems because they have simpler transceiver structure than narrowband transceivers.

Chapter 2 – UWB Localization

The capability of high-precision localization has been one of the attractive application fields of UWB technology due to the fine time resolution of UWB signals. This chapter aims to review and analyze four different techniques to estimate the location of target nodes (transmitters) using UWB signaling.

There are three main types of UWB localization techniques: signal-strength based, direction based, and time based approaches. For these three techniques, the target location is estimated by using the received signal strength (RSS), angle-of-arrival (AOA), and time-of-arrival (TOA), respectively [6].

The Time Difference of Arrival (TDOA) method which is derived from TOA is commonly concluded as the best candidate method for the target application, centimeter-accuracy 3D real time localization of multiple sources.

2.1 Received Signal Strength (RSS)

With RSS technique, the distance between two nodes can be estimated by measuring the signal strength of the object to be positioned at each receiver [6] [7]. Figure 2.1 shows how the location can be estimated using distance-based approach. Signal power is commonly expressed as

$$P(d) = \frac{1}{T}\int_0^T |r(t,d)|^2 \, dt \, , \qquad (2.1)$$

where $r(t,d)$ is the received signal at distance d and T denotes the integration interval. As a signal power decays with distance, the RSS at a node carries information about the range between the two nodes, when one of them has transmitted the signal. In order to translate the RSS information into a distance estimate, we should know the relation between signal power and distance. The distance between the nodes can be obtained from the RSS measurement at one of the nodes assuming that the transmitted signal power is known.

Path loss is one factor that affects the signal power which is reduced as a signal propagates through space. A general model for path loss is described as

$$\overline{P}(d) = P_0 - 10n\log(\frac{d}{d_0}), \qquad (2.2)$$

where n is the path-loss exponent, $\overline{P}$ denotes the average received power in decibels at a distance d, and P_0 represents the received power in decibels at a reference distance d_0 [8]. Although the path loss model shows a simple relation between distance and average signal power, it is quite complicated to get the exact relation between them in a practical wireless environment due to varying propagation mechanisms such as scattering, diffraction, and reflection, which can cause significant distortion in RSS even over small time intervals and/or short distance. The RSS technique is simple to implement, but RSS is the least appropriate method in case of UWB because it does not exploit the fine space-time resolution of pulsed signals and requires a site-specific path loss model. Additionally, RSS circuits and transmission power will vary from device to device depending on the manufacturing process. Moreover, power source depletion may change the transmitted power. Consequently, the signal strength is not a dependable parameter for location estimation using UWB signals.

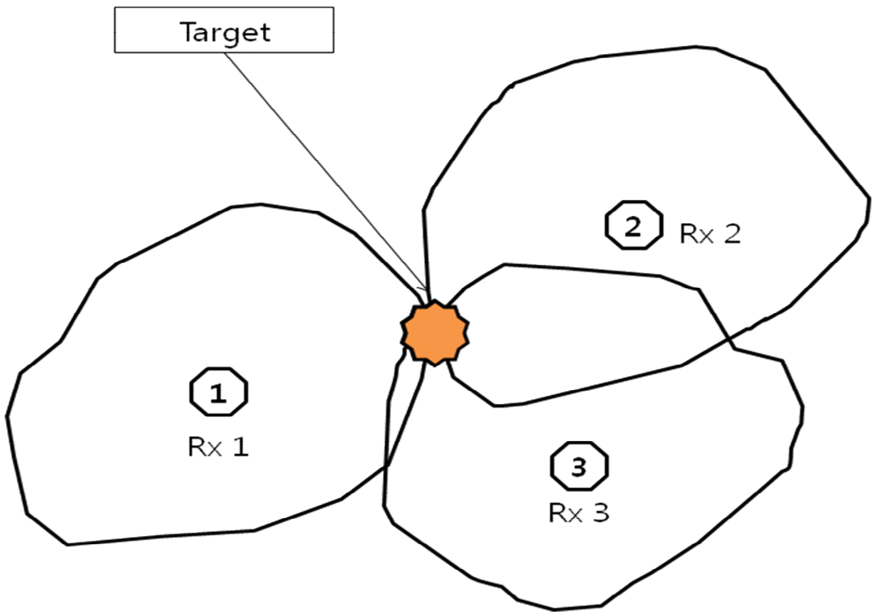

Figure 2.1: Received Signal Strength (RSS), (solid line denotes the signal strength curve related to each receiver)

2.2 Angle of Arrival (AOA)

AOA is defined as the angle between the propagation directions of incident waves. The receiver receives a signal and recognizes the direction where the signal comes from. By sharing information on the direction rather than distance of neighboring nodes, the measurements provide location information as shown in Figure 2.2. However, one common approach to AOA measurements is to use an antenna array. This means the AOA method requires multiple antennas (or at least one antenna capable of beamforming) at the receiver. This requirement leads to size and complexity demands that are often incompatible with the low-cost, small-size constraints associated with applications that UWB technology is particularly suited for [6]. In addition, multipath reflections may significantly deteriorate the accuracy of localization, especially in indoor environments. Thus, accurately estimating an angle is a challenge due to scattering of objects in dense multipath indoor environments [7].

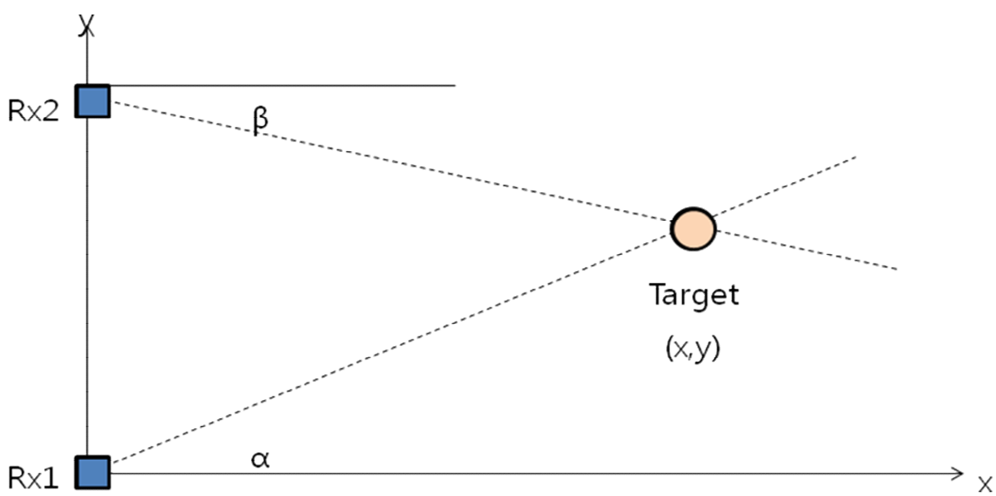

Figure 2.2: Angle of Arrival (AOA)

2.3 Time of Arrival (TOA)

TOA and Time-difference-of-arrival (TDOA) are the positioning methods related to the time at which the signal has been received at the receiver from the transmitter whose location is to be estimated. Time based approaches are considered the proper ones to be employed for the UWB localization, since the fine-time resolution of the pulsed signal will facilitate accurate detection of the arrival time instants of the received signal [6] [9]. From this precise TOA information, a time-based approach gives results of more accurate positioning estimation than those of other methods such as RSS and AOA. In this section, we focus on the TOA method: how it works to estimate the location.

In the TOA scheme, the flight time of the signal from the transmitter to the receiver is used for calculating the distance between the Tx and Rx using the speed of light as shown in Figure 2.3. For example, a target node transmits a signal through a certain wireless channel at time t_{trs} and the receiver receives this signal at time t_{rcv}. The flight time of the signal is $t_{rcv} - t_{trs}$, and the distance between Tx and Rx is d = ($t_{rcv} - t_{trs}$)*c, where c is speed of light 299,792,458 m/s. Note that t_{trs} and t_{rcv} are the real common time instants rather than the local time instants from the independent local clocks of each receiver. Actually, each wireless node (both receivers and the transmitter) has an independent local clock and the arrival time instant must be detected in terms of its local clock rather than the real common clock. Therefore, this timing concept causes some synchronization issues.

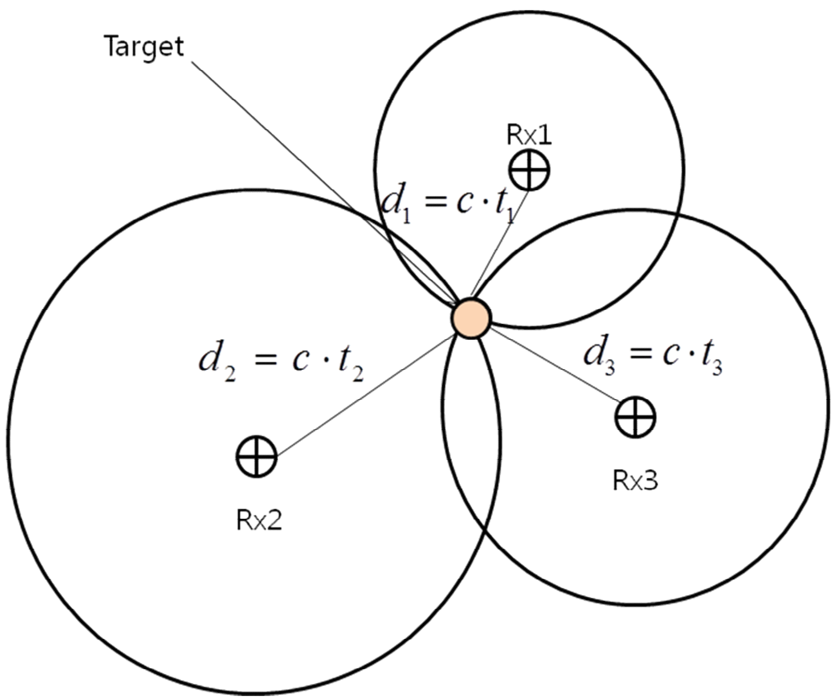

Figure 2.3: Time of Arrival (TOA)

In order to estimate the precise distance between the transmitter and the receiver, both nodes must have a common clock, i.e., the transmitter and receiver must have a synchronized timing clock in the TOA method. However, transmitter-receiver synchronization is challenging to achieve because the transmitter is located at an unknown position and could be moving around randomly. If the transmitter is moving around, the propagation delay which is an important factor to compute the clock offset is difficult to estimate. This difficulty makes timing synchronization for TOA challenging as shown in Figure 2.4. To avoid the synchronization issue, the TDOA technique will be used as described in the next section.

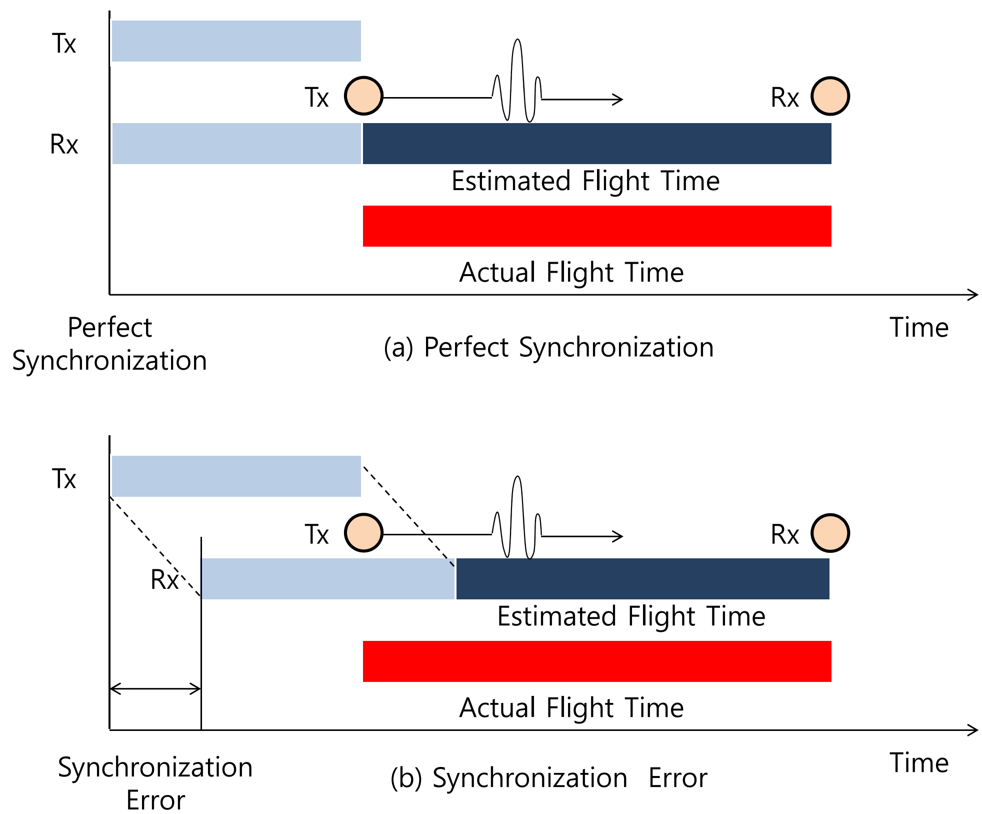

Figure 2.4: (a) Perfect Synchronization (b) Synchronization error

2.4 Time Difference of Arrival (TDOA)

The TDOA scheme is based on estimating the difference in the arrival times of the signal between the synchronized receiver nodes. These time instants are converted to distance by the speed of light, the same as in the TOA method. The TDOA scheme, however, does not require knowledge of the absolute time of the transmission like the TOA scheme; only synchronization among receiver clocks is needed [10]. The TDOA of two signals traveling between the target node and two reference nodes is estimated, which determines the location of the node on a hyperbola, with foci at the two reference nodes [6] [7].

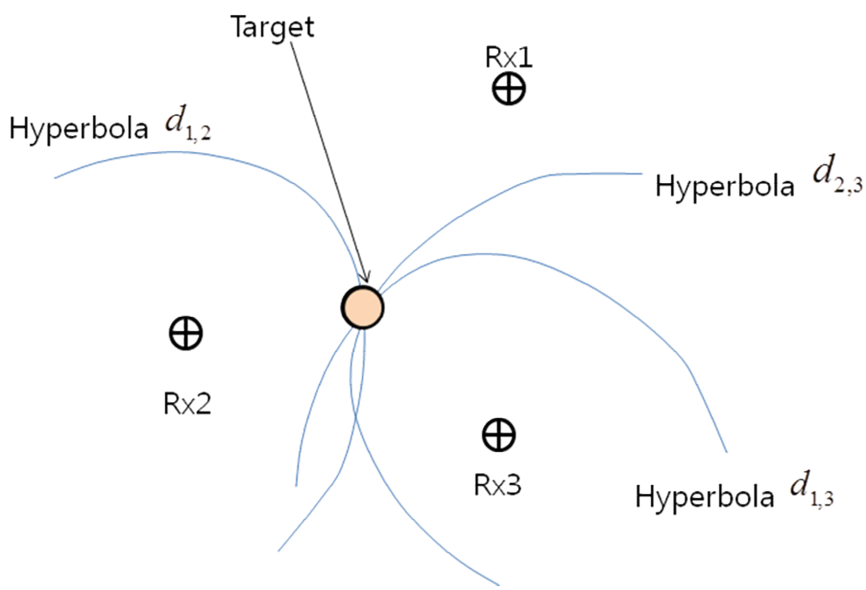

Figure 2.5: Time Difference of Arrival (TDOA)

For 2-D localization, a third reference node is needed. The non-linear hyperbolic equation for TDOA method is described as:

$$d_{j,k} = \sqrt{(x_i - x_j)^2 + (y_i - y_j)^2} - \sqrt{(x_i - x_k)^2 + (y_i - y_k)^2} \qquad (2.3)$$

where $d_{j:k}$ is the range difference obtained from the estimated TDOA, (x_i, y_i) is the coordinate of the target node, which is at an unknown position, and (x_j, y_j) and (x_k, y_k) are the coordinates of the receiver nodes that have known positions. Figure 2.5 employs Eq. (2.3) to find the hyperbolas from two reference nodes. Thus, we can determine one crossing point of two hyperbolas from three receivers and the point is the estimated position of the target node. Since TDOA can be estimated by comparing TOA at each receiver, time information of the transmitter does not affect TDOA estimation as shown in Figure 2.6. Therefore, TDOA technique is regarded as the best method for UWB localization if the target is required to be extremely simple.

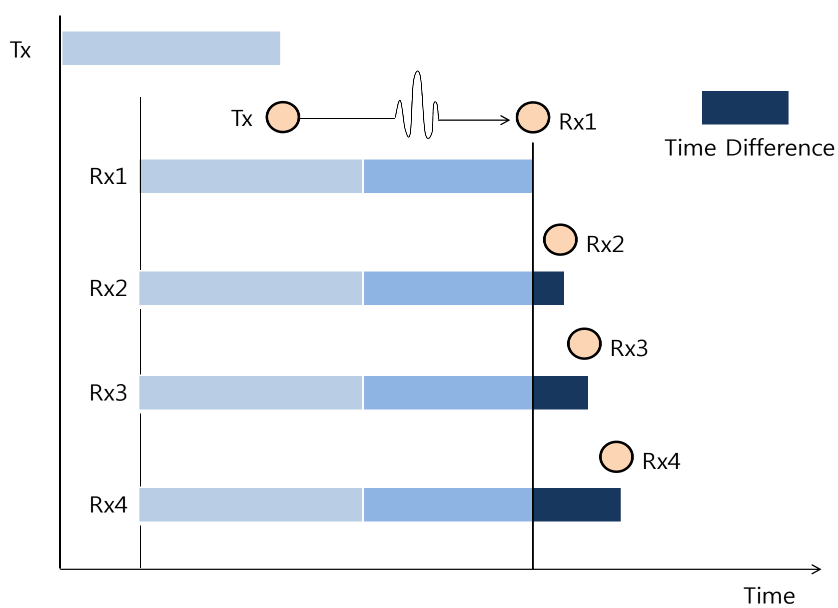

Figure 2.6: Time differences between receivers

Chapter 3 – Signal Design for Multiple Source Localization

Multiple transmitters each send a distinct signal which has characteristic high-value auto-correlation and low-value cross-correlation. This is used to separate each intended signal among mixed signals at the receivers. Therefore the transmitted signal should be designed to maximize such properties for better localization results. In this thesis, Gold codes are chosen as the best candidate for localization of multiple sources. Note that the application of the codes generated is different from that of common communications systems. In general, Gold codes are used in spread spectrum systems which rely on spreading codes to create noise-like transmissions. Spread spectrum systems have transmitted signals that are spread over a frequency band much wider than the minimum bandwidth needed to transmit the intended information [3].

Because the spread spectrum signal has a much wider bandwidth than narrowband receivers in the same range and requires a knowledge of the wideband encoding method to demodulate it, it is not intercepted by, or does not severely interfere with narrowband systems due to little power falling in the bandpass of any given narrowband receiver. Figure 3.1 shows how a gold sequence works. The original information is modulated with a code sequence.

The use of Gold codes in the thesis is different from the use of spread spectrum in narrowband communication systems because UWB signals occupy an ‘ultra wide’ band. The pulsed UWB signals with unique codes propagate to a minimum of four receivers. The received signals are correlated with each code at the server and the positions of multiple sources are calculated through a TDOA localization method from the information on time differences of receivers.

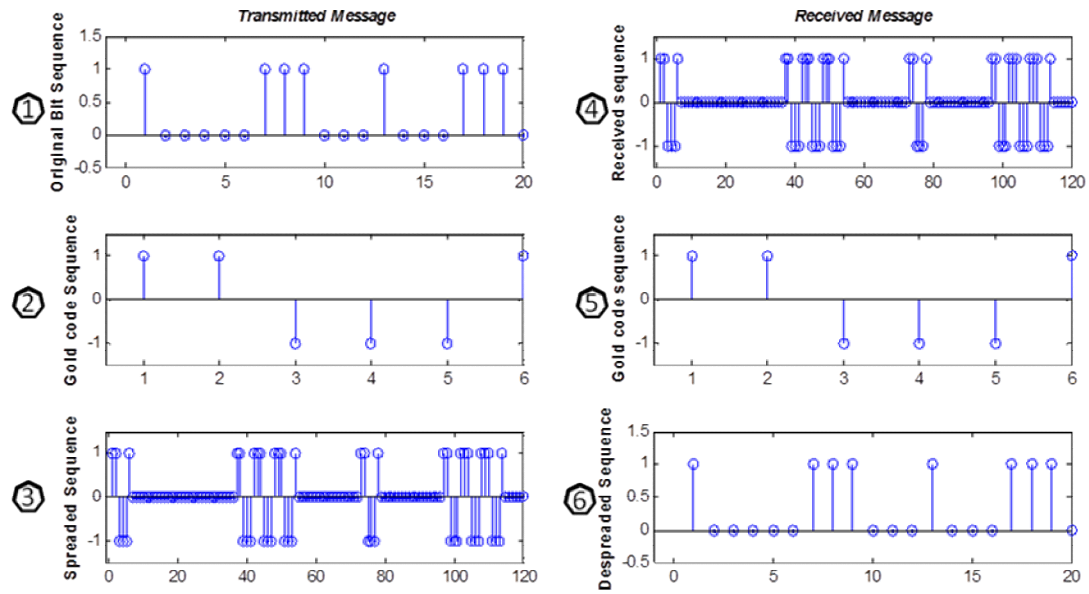

Figure 3.1: Usage of 6-bit gold code (coded and decoded) in spread-spectrum communications; transmit sequences (3) have longer sequences in length than those in the original one (1) because the original sequences are encoded with a set of Gold code (2). Decoding process is shown from (4) to (6).

3.1 Code Design

The set of codes used for multiple sources (users) should have as little mutual interference as possible and as high self-identification as possible as well. Gold sequences because a large quantity of codes are easily generated and have the desired properties of low cross-correlation and high autocorrelation values compared to the others [11]. To further reduce mutual interference, a subset of the Gold sequences with very low cross-correlation values will be chosen.

3.1.1 Generation of Gold Codes

Gold codes can be constructed from a modulo-2 addition of two maximum length sequences (m-sequence). The code sequences are added chip by chip by synchronous clocking. The generated codes are of the same length as the two base codes, which are added together as given in Figure 3.2 [12].

The codes of the length of 31 (= 2^5-1) are generated by the process above as follows:

Sequence 1 : 1111100110100100001010111011000

Sequence 2 : 1111101100111000011010100100010

0 shift combination set: 0000001010011100010000011111010

1 shift combination set: 0000111111010100111111110011101

…

30 shift combination set: 1000010000111000000111101001001

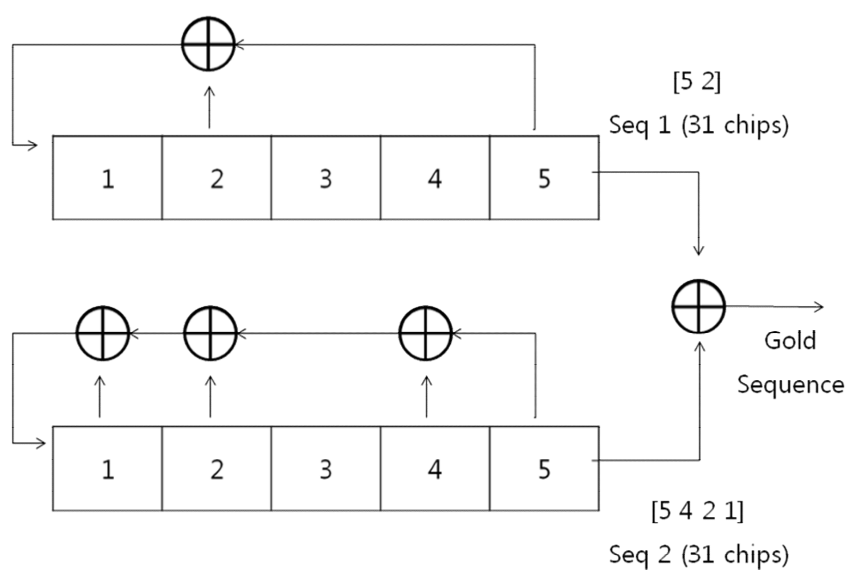

Figure 3.2: Generation of Gold code set

The N+2, 33 in this example, elements of the Gold code set are generated by this process. In the thesis, 10 Linear Feedback Shift Registers (LFSRs) are used to generate 1025 codes with a length of 1023 (= 2^{10}-1). The codes generated in the simulation are slightly different from the example above in terms of pulse amplitude, for example -1,1,1,-1,-1 instead of 0,1,1,0,0. The pulsed UWB can be represented as:

$$p_1(t) = \sum_{i=0}^{N-1} g_1^{i+1} w(t - iT), \tag{3.1}$$

where $p_1(t)$ is the pulsed UWB signal, g_1 denotes the code #1 (length of 1023), and w(t) represents the Gaussian pulse with duration of 1 ns. The pulsed UWB of sequence -1,1,1,-1,-1 is expressed in Figure 3.3. The original sequences are upsampled by 100 such that the code becomes -1,0,0…(99 zeros),1,0,0…,1,0,0,…,-1,0,0,…-1,0,0,…0 as shown in Figure 3.4. So transmitting one set of the code #1 takes about 100 μs (= 1ns X 1023 X 100) .

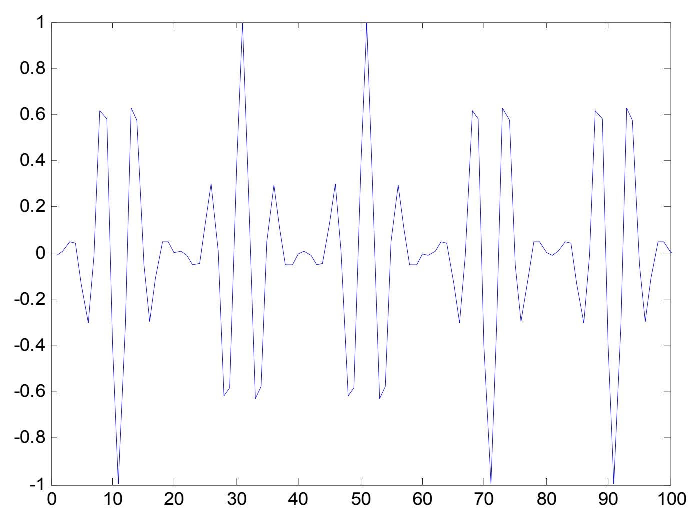

Figure 3.3: The pulsed UWB signal of sequence '-1,1,1,-1,-1'

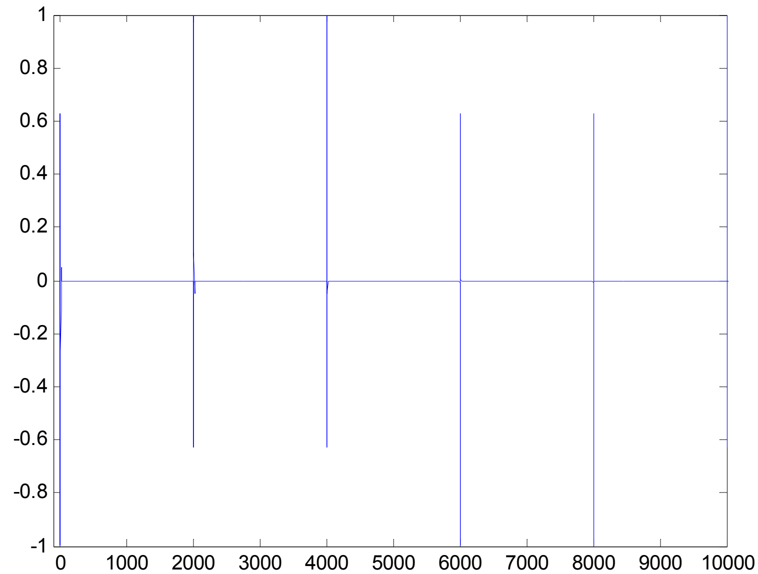

Figure 3.4: The pulsed UWB signal of sequence '-1,1,1,-1,-1'upsampled by 100

3.1.2 Properties of Gold Code

Correlation properties of codes take a major part in the code design for multiple sources since they determine the degree of multiple access interference and the code acquisition properties. Correlation determines how much similarity one set of code has with others.

The autocorrelation function determines how much a sequence is similar to a phase-shifted version of itself [13] [15] and is expressed as

$$R_{XX}(t,t+\tau) = E[X(t)X(t+\tau)], \tag{3.2}$$

$$R_{XX}(t,t+\tau) = \frac{1}{2T}\int_{-T}^{T} f_X(t) f_X(t+\tau)dt , \tag{3.3}$$

$$R(\tau) = \frac{1}{N} \sum_{i=1}^{N} X_i X_{i-\tau} \,, \tag{3.4}$$

where R_{XX} is the autocorrelation function, T and N denotes the period of time (continuous and discrete respectively), and τ is the delay time (or lag time).

The autocorrelation of Gold codes has a single peak at the center (zero) like PN sequences as shown in Figure 3.5 in the simulation. Gold sequences in use allow the transmission to be asynchronous because the receiver can synchronize properly using the autocorrelation property of the Gold code.

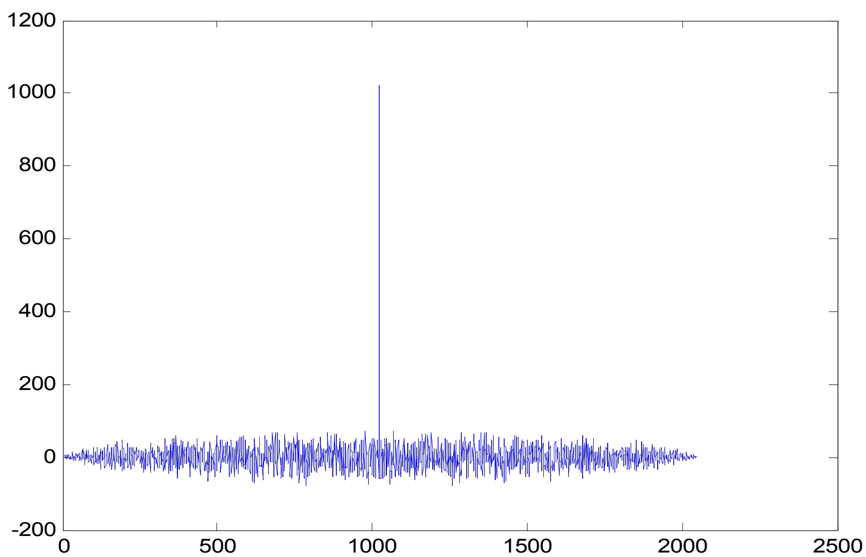

Fig. 3.5: The autocorrelation of a code

One of the advantages of Gold codes is that a large number of codes can be generated easily. The Gold codes are selected so that the autocorrelation and cross-correlation between different codes are uniform and bounded over a set of codes available from a given generator. The generated Gold codes have three cross-correlation values as given in Table 3.1 [12] [14], which decrease as the length of the code increases.

Shift-Register Length (m)	Period (Code length)	Values of Cross-Correlation
Odd	$N = 2^m - 1$	$-1/N$, $-(2^{(m+1)/2}+1)/N$, $(2^{(m+1)/2}+1)/N$
Even (not divisible by 4)	$N = 2^m - 1$	$-1/N$, $-(2^{(m+2)/2}+1)/N$, $(2^{(m+2)/2}+1)/N$

Table 3.1: Cross-correlation properties of Gold sequences

Cross-correlation measures essentially how similar two different sequences are when one of them is shifted in phase relative to the other [13] [15] and is represented by

$$R_{XY}(t, t+\tau) = E[X(t)Y(t+\tau)], \tag{3.5}$$

$$R_{XY}(t, t+\tau) = \frac{1}{2T}\int_{-T}^{T} f_X(t) f_Y(t+\tau)dt, \tag{3.6}$$

$$R_{X,Y}(\tau) = \frac{1}{N}\sum_{i=1}^{N} X_i Y_{i-\tau}, \tag{3.7}$$

where R_{XY} represents the cross-correlation function.

3.1.3 Algorithm to select a subset of optimized codes from Gold codes

To achieve better positioning results with multiple sources, Gold codes need to be sorted out in order of the value of cross-correlation. To do so, the cross-correlation of a whole set of Gold codes generated should be calculated and compared to the average value of cross-correlation of every single code to the others as described in Table 3.2. Code 2 and Code 1024, for instance, are chosen as optimized codes because the two codes produce the smallest cross-correlation values as in Table. Code 2 and Code 3, then, have the second least value. In case duplicate code exists, only Code 3 is selected. Consequently, the sorting process results in a subset of 200 out of a set of 1025 codes generated with 10 Linear Feedback Shift Registers.

3.2 Path Loss Model

The path loss of a conventional narrowband system is defined as [8]

$$PL(d) = \frac{E\{P_{RX}(d, f_c)\}}{P_{TX}}, \tag{3.8}$$

where P_{TX} is the transmit power, P_{RX} denotes the received power as seen at the antenna of transmitter and receiver, respectively, and d represents the distance between transmitter and receiver. f_c is the center frequency and the expectation $E\{\cdot\}$ is taken over a range that is large enough to allow averaging out of the shadowing effects. It is well known that the median of path loss is directly proportional to d raised to some exponent γ. The path loss (dB) at some distance d is described by [16]:

$$PL(d) = PL_0 + 10\gamma \log_{10}(\frac{d}{d_0}) + S(d); d \geq d_0 = 1m, \tag{3.9}$$

where the reference distance d_0 is set to 1m, PL_0 represents the path loss at the reference distance, γ denotes the path loss exponent which depends on the environment and on whether a line-of-sight (LOS) connection exists between the transmitter and receiver or not. S (dB) is the lognormal shadow fading component which is a zero mean Gaussian random variable with standard deviation σ in dB. The statistical values of the path loss model parameters are summarized in Table 3.3 [16]. In the simulation, only the LOS parameters are considered.

Code #	1	2	3	…	1024	1025
1		15.9888	17.4763	…	16.8572	16.6714
2			15.3501	…	17.8900	13.3022
…						
1024						16.3213
1025						

Table 3.2: The process of selecting optimized codes among a set of 1025 Gold codes

	LOS		NLOS	
	Mean	**Std. Dev.**	**Mean**	**Std. Dev.**
PL_0 **(dB)**	47	N/A	50.5	N/A
γ	1.7	0.3	3.5	0.97
σ **(dB)**	1.6	0.5	2.7	0.98

Table 3.3: Statistical values of the path loss model parameters [16]

3.3 Estimator

The TDOA equation expressed in coordinates (x, y, z) is [17]

$$f_i = \sqrt{(x_{i,1} - x_u)^2 + (y_{i,1} - y_u)^2 + (z_{i,1} - z_u)^2} - \sqrt{(x_{i,2} - x_u)^2 + (y_{i,2} - y_u)^2 + (z_{i,2} - z_u)^2} , \tag{3.10}$$

where $(x_{i,1}, y_{i,1}, z_{i,1})$ and $(x_{i,2}, y_{i,2}, z_{i,2})$ are the coordinates of the two receivers at the i^{th} time interval and (x_u, y_u, z_u) is the unknown target coordinate [18]. By plugging an actual position in equation (3.10) with the estimated position, $(\hat{x}_u, \hat{y}_u, \hat{z}_u)$, the approximated TDOA can be described as

$$\hat{f}_i = \sqrt{(x_{i,1} - \hat{x}_u)^2 + (y_{i,1} - \hat{y}_u)^2 + (z_{i,1} - \hat{z}_u)^2} - \sqrt{(x_{i,2} - \hat{x}_u)^2 + (y_{i,2} - \hat{y}_u)^2 + (z_{i,2} - \hat{z}_u)^2} , \tag{3.11}$$

where

$$\begin{aligned} x_u &= \hat{x}_u + \Delta x_u \\ y_u &= \hat{y}_u + \Delta y_u \\ z_u &= \hat{z}_u + \Delta z_u \end{aligned} \tag{3.12}$$

Expanding the Taylor Series around $(\hat{x}_u, \hat{y}_u, \hat{z}_u)$ and retaining the first order term lead to

$$\Delta f_i = \frac{\partial f_i}{\partial \hat{x}_u}\Delta x_u + \frac{\partial f_i}{\partial \hat{y}_u}\Delta y_u + \frac{\partial f_i}{\partial \hat{z}_u}\Delta z_u\,, \tag{3.13}$$

where

$$\Delta f_i = f_i - \hat{f}\,, \tag{3.14}$$

$$\frac{\partial f_i}{\partial \hat{x}_u} = -\frac{x_{i,1} - \hat{x}}{\hat{r}_i} + \frac{x_{i,2} - \hat{x}}{\hat{r}_i}\,, \tag{3.15}$$

$$\hat{r}_i = \sqrt{(x_{i,1} - \hat{x}_u)^2 + (y_{i,1} - \hat{y}_u)^2 + (z_{i,1} - \hat{z}_u)^2} - \sqrt{(x_{i,2} - \hat{x}_u)^2 + (y_{i,2} - \hat{y}_u)^2 + (z_{i,2} - \hat{z}_u)^2}\,. \tag{3.16}$$

With n TDOA measurements, equation (3.14) is expressed as a linear model in the matrix form as

$$\boldsymbol{\Delta f} = \mathbf{H}\boldsymbol{\Delta\chi},$$

where

$$\Delta\boldsymbol{f} = \begin{bmatrix} \Delta f_1 \\ \Delta f_2 \\ \vdots \\ \Delta f_k \end{bmatrix}, \tag{3.17}$$

$$\mathbf{H} = \begin{bmatrix} \frac{\partial f_1}{\partial \hat{x}_u} \frac{\partial f_1}{\partial \hat{y}_u} \frac{\partial f_1}{\partial \hat{z}_u} \\ \frac{\partial f_2}{\partial \hat{x}_u} \frac{\partial f_2}{\partial \hat{y}_u} \frac{\partial f_2}{\partial \hat{z}_u} \\ \vdots \\ \frac{\partial f_n}{\partial \hat{x}_u} \frac{\partial f_n}{\partial \hat{y}_u} \frac{\partial f_n}{\partial \hat{z}_u} \end{bmatrix}, \tag{3.18}$$

$$\boldsymbol{\Delta\chi} = \begin{bmatrix} \Delta x_u \\ \Delta y_u \\ \Delta z_u \end{bmatrix}, \tag{3.19}$$

The location of the target can be obtained by carrying an iterative least square estimate where the location of the target is updated by iteration of Eq. (3.12). In the simulation 3,000 iterations of least square are carried out to minimize the position error.

3.4 Simulation

3.4.1 Simulation setup for single source

The simulation begins with one transmitter located at [2, 3, 7] in a room with a size of 1,000 cubic meters (10m X 10m X 10m). There are four receivers set at the corners of the room, whose coordinates are R1 [0, 0, 0], R2 [10, 10, 0], R3 [10, 0, 10], and R4 [0, 10, 10] as shown in Figure 3.6.

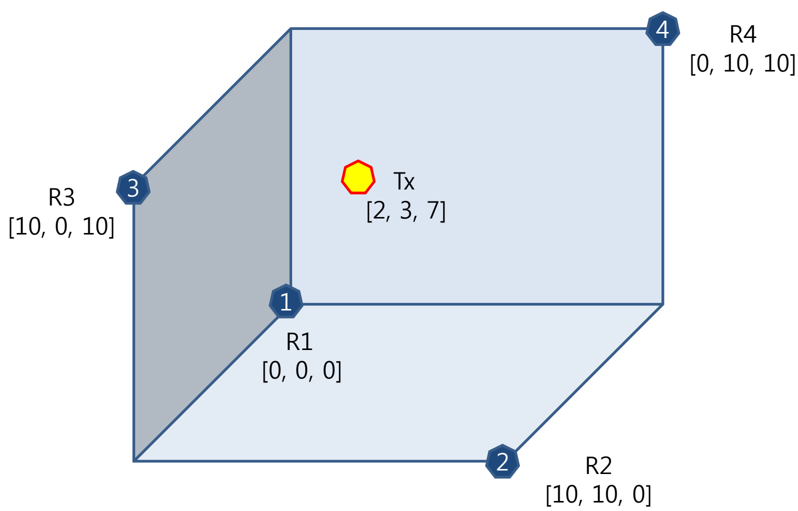

Figure 3.6: Simulation setup of a transmitter and receivers

A transmitted signal with the unique code reaches each receiver at a different time depending on the distance between the source and receivers. The strength (or weakness) of the received signal depends on the distance-based path-loss model which is stated in Section 3.1.2 and determines the peak of correlation at each receiver as shown in Figure 3.7. The time differences between the peaks of the correlation function form the three hyperbolic curves from four receivers. The time differences between receivers are shown in Table 3.4.

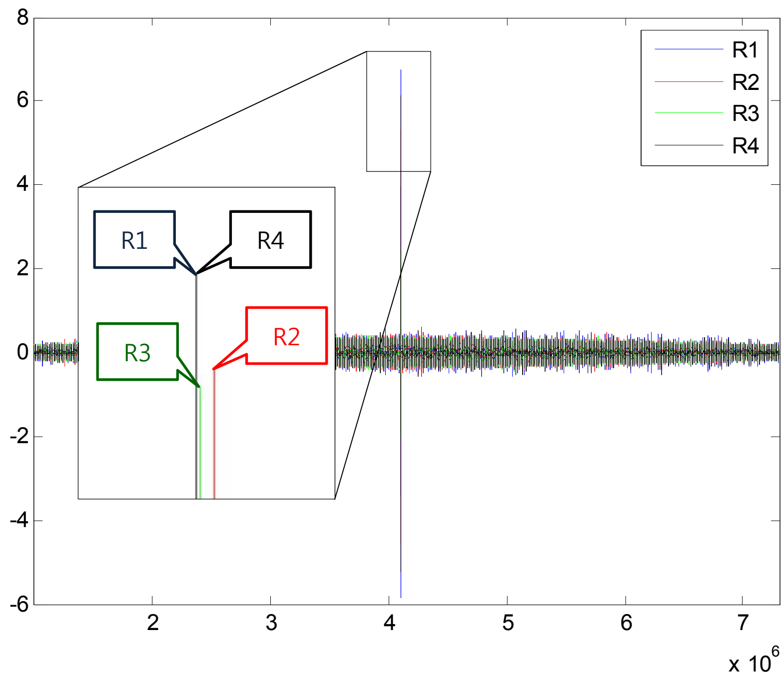

Figure 3.7: Peaks of correlation

Table 3.4 explains the time differences between each receiver as shown in Figure 3.7. A signal reaches Receiver 1 and Receiver 4 first at the same time, then Receiver 3 and Receiver 2. Time difference between Receiver 1 and Receiver 2 is 40.5 ns, and the time difference between Receiver 1 and Receiver 3 is 9.88 ns. Note that the time difference between Receiver 1 and Receiver 4 is zero. This means that a single source is located at the same distance from these two receivers.

Unit (ns)	R1	R2	R3	R4
R1	0	40.5	9.88	0
R2		0	30.63	40.5
R3			0	9.88
R4				0

Table 3.4: The time differences between each receiver

In Figure 3.7, the peaks of correlation indicate the distances between each receiver and the source, which are Receivers 1 and 4 (the same distance), Receiver 3, and Receiver 2 in order of distance. However, the peak of Receiver 2 has a higher value than the one of Receiver 3 with a longer distance though because the path-loss model contains a random shadowing component with standard deviation σ in dB as shown in Table 3.3 of Section 3.1.2. The position result from the process is [1.999, 3.000, 6.999].

3.4.2 Simulation setup for multiple sources

With a large number of sources, transmit codes are selected from optimized codes sorted in Section 3.1.3. The server takes the received signals from four receivers and correlates with all codes it has and calculates the delay time of each code from correlation process, which comes from the unique autocorrelation property of single peak at the center (zero) as stated in Section 3.1.2. Other codes function as interference and noise to the desired code as shown in Figure 3.8.

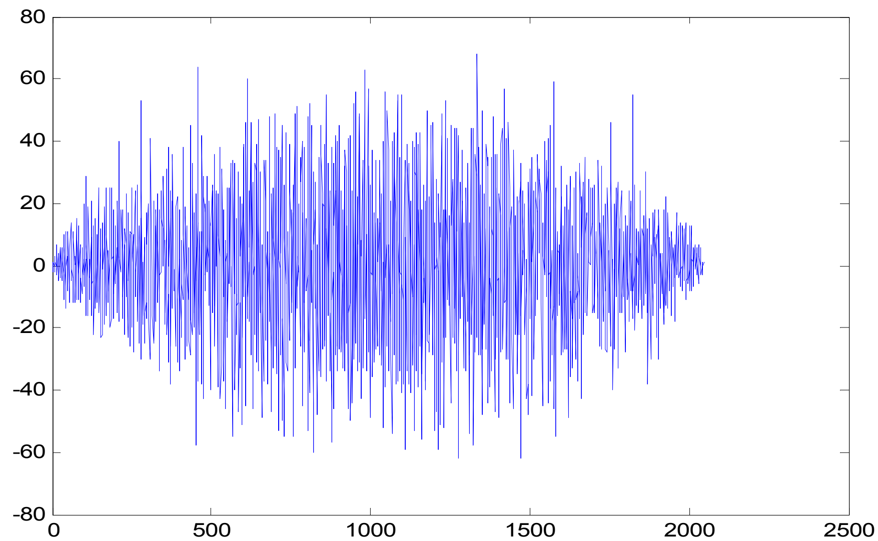

Figure 3.8: The cross-correlation of two different codes

The positions of 10 transmitters are shown in Table 3.5.

Tx	*AP	**EP	Tx	AP	EP
1	[3, 6, 6]	[3.000, 5.999, 5.999]	6	[2, 7, 7]	[2.002, 6.999, 6.999]
2	[8, 2, 2]	[8.000, 1.999, 1.999]	7	[4, 7, 6]	[4.000, 6.999, 5.999]
3	[8, 7, 3]	[7.998, 6.999, 3.000]	8	[8, 4, 4]	[8.000, 3.999, 3.999]
4	[5, 8, 2]	[5.000, 8.000, 1.999]	9	[7, 6, 8]	[7.000, 6.000, 8.000]
5	[7, 6, 2]	[7.000, 6.000, 1.998]	10	[8, 3, 2]	[8.001, 2.999, 1.998]

* AP : Actual position; EP : Estimated position

Table 3.5: Position results of 10 transmitters

Chapter 4 – Experiments

4.1 Experiment Setup

Bearing in mind the accurate localization results of the simulation, an experiment is carried out to determine the capabilities of the system in a real-world environment, such as a warehouse. The experiment is conducted in a building as shown Figure 4.1. The experiment consists of three main parts: signal transmitters, receivers and a server. Specific experimental devices will be discussed in following sections.

4.1.1 Transmitter

The transmitter part is composed of the code generator with length of 1023 and the Gaussian pulse generator with pulse width of 1ns in this thesis as shown in Figure 4.2. Both waveforms are generated by using MATLAB and SIMULINK. Pulses are transmitted by an Arbitrary Waveform Generator (AWG), AWG7122B, which has a sampling rate of 12GS/s and amplified by a Minicircuits ZX60-6013E-S+ power amplifier. AWG 7122B is limited to two output channels, and thus can only act as two transmitters.

Figure 4.1: Experiment building (building located in Corvallis, Oregon)

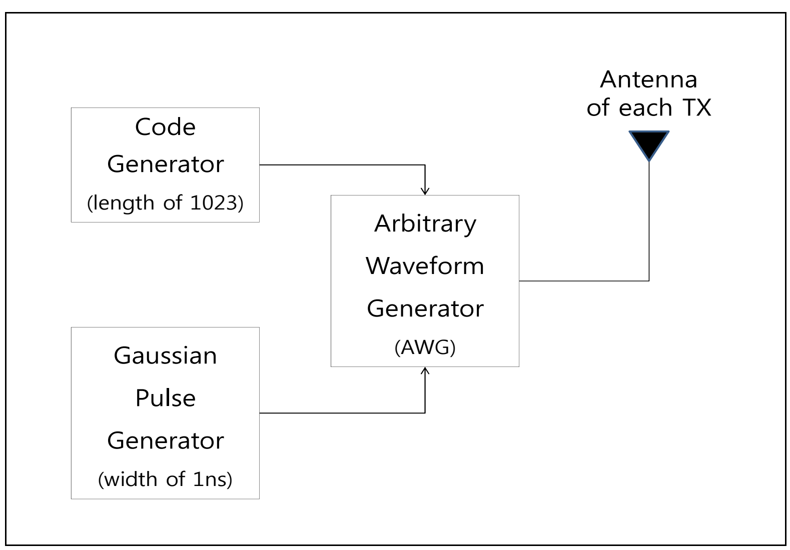

Figure 4.2: Block diagram of the transmitter

Due to this limitation, we use one of two channels to transmit an ‘intended’ signal and the other channel as interference; that is, a set of 99 codes are mixed up and act as a noise at the center of the receiver antenna configuration. Interference signals are transmitted in two different ways – symbols occur at the same time (Case 1) and at different times, to be determined randomly (Case 2) as described in Figure 4.3. Consequently, a total of 100 signals are transmitted from two different positions and transmitters. The transmitters’ location of the intended signal and interference source are described in Table 4.1. The exact locations of transmitters are measured by a laser localization system.

Four receivers are installed in the building as described in Table 4.2. The exact positions of receivers are also measured by the laser localization system.

Trial	Case 1 [x, y, z] (m)			Case 2 [x, y, z] (m)		
1	1.1062	2.09013	0.71849	0.8601	2.06799	0.71761
2	1.86562	2.18403	1.55071	1.99542	2.11736	1.54984
3	0.77025	0.69833	0.71794	0.95684	0.55336	0.71608
4	1.84829	0.51071	1.54713	2.17231	0.63291	1.54857
Interference	1.63176	1.29331	1.07437	Same as left		

Table 4.1: The transmitter’s position of intended signal and interference source

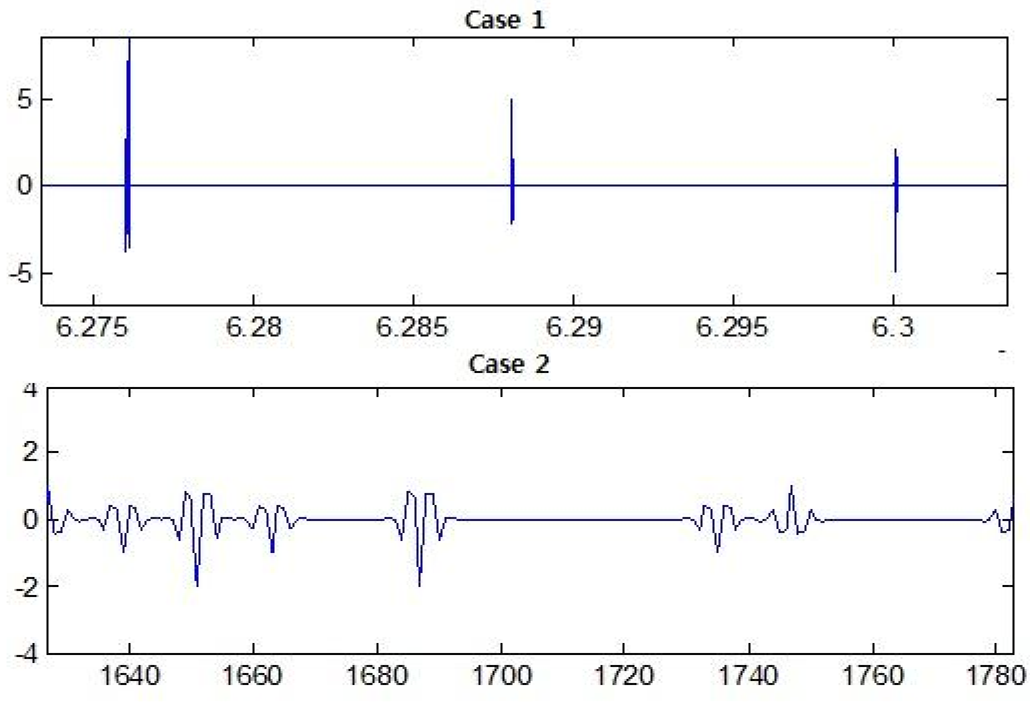

Figure 4.3: Signals transmitted at the same time (Case 1), at different time (Case 2)

4.1.2 Receiver

Rx	Coordinate (m)		
1	0	0	0
2	-0.01040	2.48750	2.30072
3	2.62271	2.46287	0.00522
4	2.56748	-0.17025	2.30192

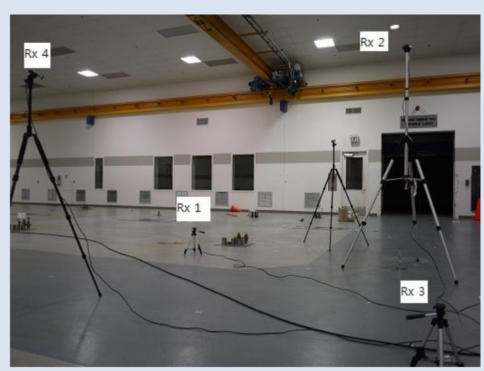

Table 4.2: The receivers' positions

The signals transmitted are distorted due to time and spatial mixing with the other signals and thermal noise through the channel. Consequently, the signals received at the receiver are not clean anymore as shown in Figure 4.4. The signals received at the receiver antennas are shown in Figure 4.5. It should be noted that a faulty lighting system emits bursts of electromagnetic energy in the bandwidth of the receivers, and therefore acts as an additional noise source.

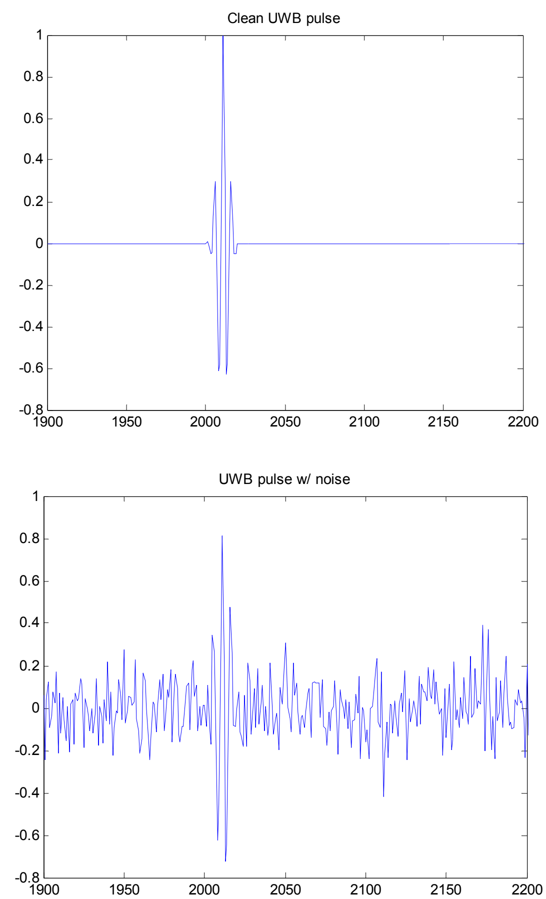

Figure 4.4: Clean UWB pulse and snapshot including noise

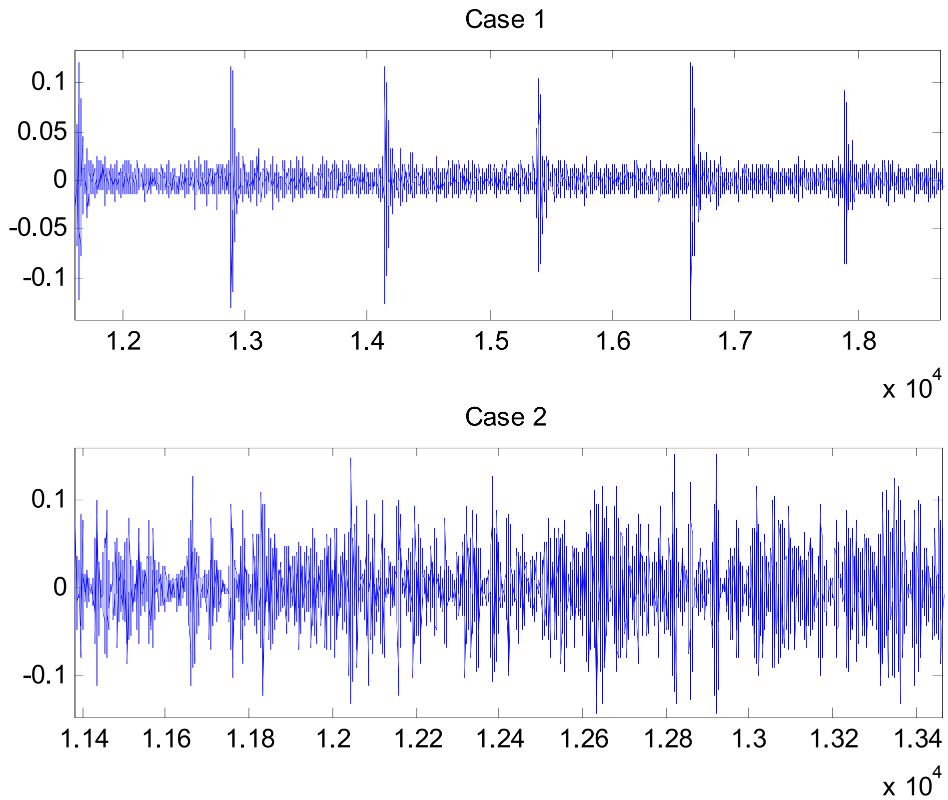

Figure 4.5: Received signals at Receiver 1 (Case 1 and Case 2)

4.1.3 Server

To carry out the experiment, various types of experimental devices are employed from the transmitter to the server as shown in Figure 4.6. The signals received at the receiver antennas are sent through cables connected to a custom amplifier structure and then to a Digital Serial Analyzer (DSA) which samples those signals and converts to numerical data. The server takes several processing stages as shown in Figure 4.7 such as correlation with original sequences to detect the exact code sent and the position estimator to find out the exact position of targets using the hyperbolas of the previously described TDOA method.

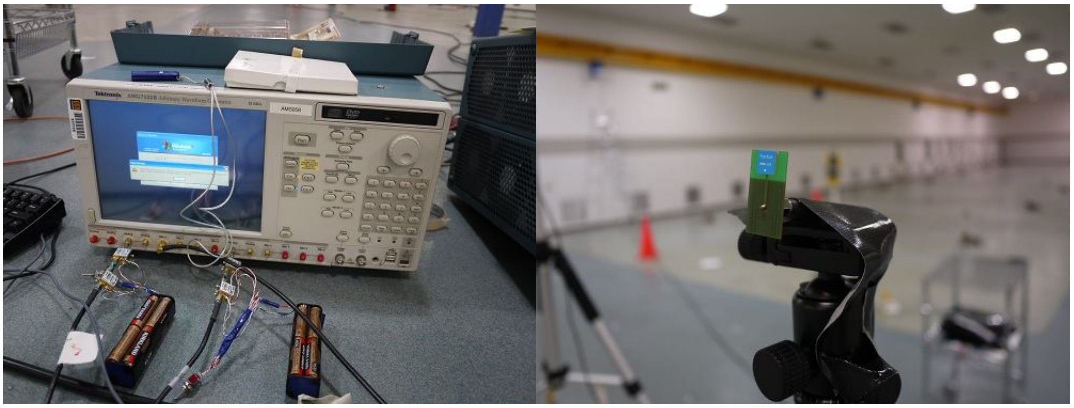

(a) Arbitrary Waveform Generator (b) Transmit and receive antenna

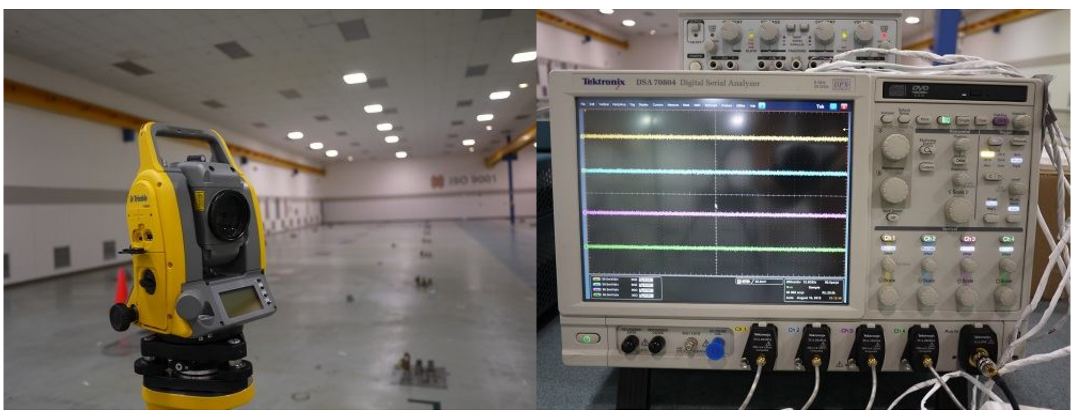

(c) Laser Rangefinder (d) Digital Serial Analyzer

Figure 4.6: Experimental devices used for the experiment

The correlation process produces values of autocorrelation and cross-correlation. As stated in Chapter 3, a set of optimized codes works in the set of mixed signals to find out its own code as shown in Figure 4.8 and Figure 4.9. The difference the instantaneous peak within the correlation function at each receiver provides the critical time difference information to the TDOA method.

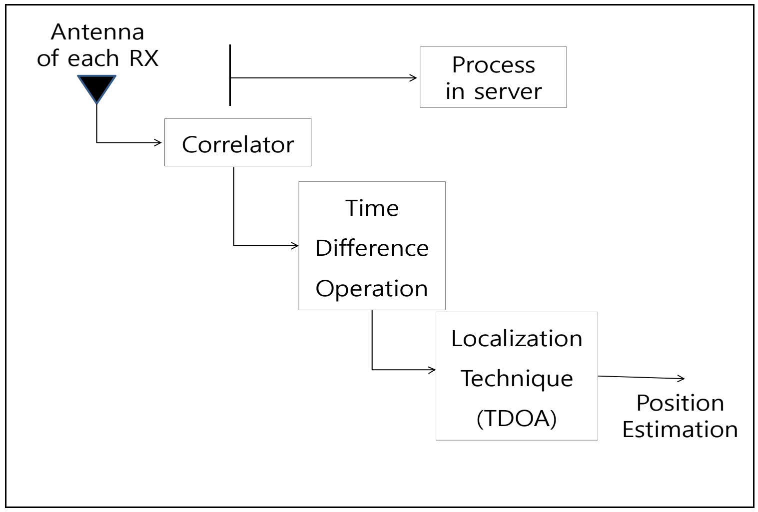

Figure 4.7: Block diagram of the receiver and server

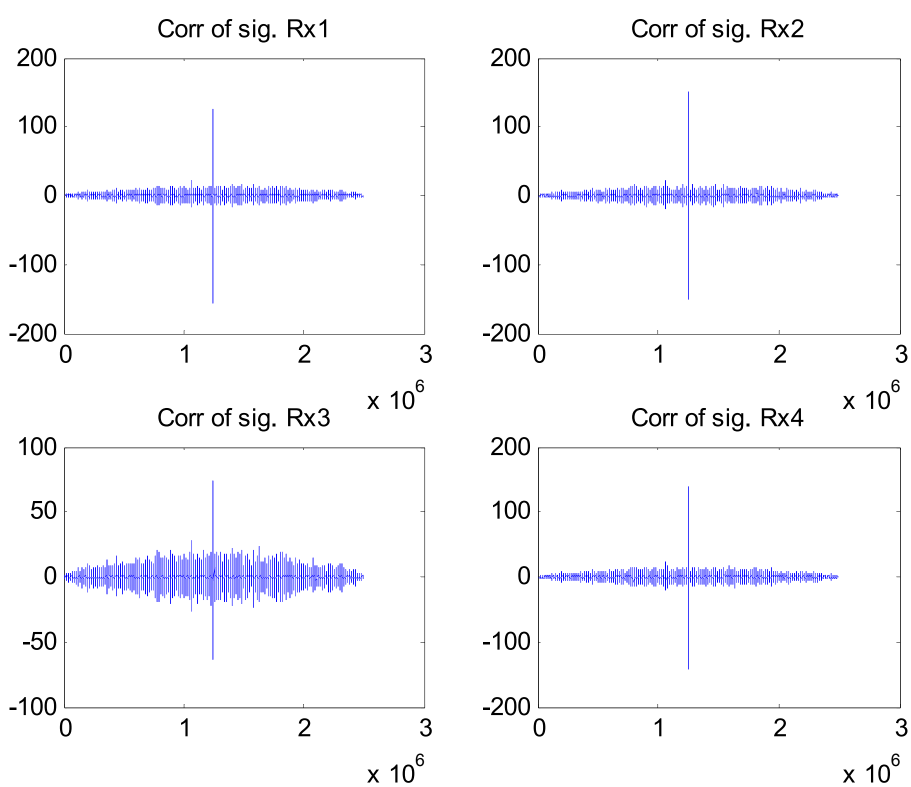

Figure 4.8: Correlation results of intended signal (Case 1)

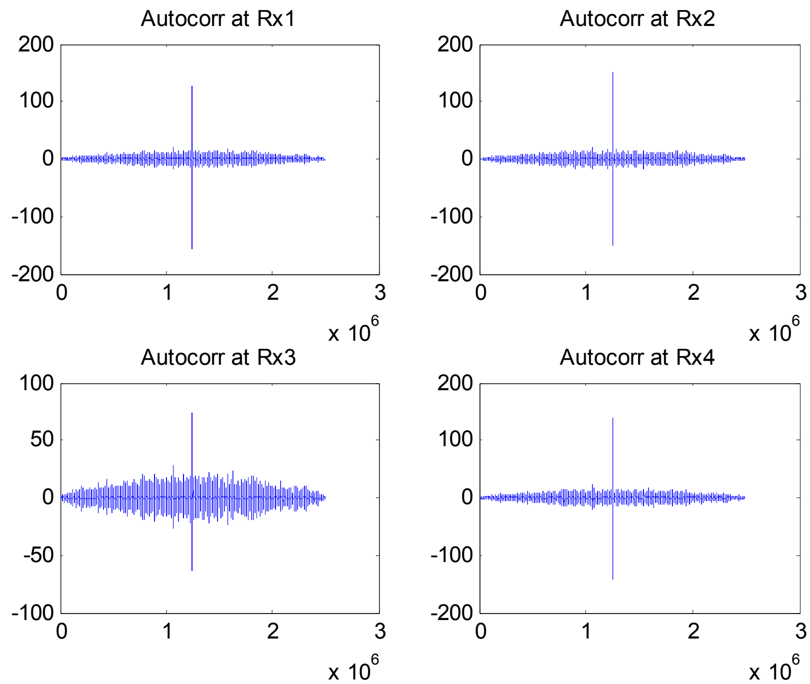

Figure 4.9: Correlation results of intended signal (Case 2)

4.2 Results

It should be noted that due to data acquisition limits, each estimation is performed on only once source correlation, with no averaging. Subsequent experiments should include averaging of position estimates to increase the accuracy from what is observed in this section.

The localization error of Case 1 ranges from 0.0363m to 0.1339m and that of Case 2 from 0.0779m to 0.2549 as described in Table 4.3 and Table 4.4, respectively.

Trial		Target Coordinate (m)			Error (m)
1	AP*	1.1062	2.09013	0.71849	0.1339
	EP**	1.03882	2.16023	0.62637	
2	AP	1.86562	2.18403	1.55071	0.0363
	EP	1.89738	2.21744	1.56508	
3	AP	0.77025	0.69833	0.71794	0.0645
	EP	0.74565	0.64103	0.70158	
4	AP	1.84829	0.51071	1.54713	0.0578
	EP	1.90188	0.49622	1.53087	

* AP : Actual Position; ** EP : Estimated Position

Table 4.3: Localization Results and Error (Case 1)

Trial		Target Coordinate (m)			Error (m)
1	AP	0.8601	2.06799	0.71761	0.2549
	EP	0.86247	2.32269	0.72653	
2	AP	1.99542	2.11736	1.54984	0.1311
	EP	2.04363	2.23584	1.57879	
3	AP	0.95684	0.55336	0.71608	0.1277
	EP	0.89423	0.45187	0.76165	
4	AP	2.17231	0.63291	1.54857	0.0779
	EP	2.22157	0.64936	1.49056	

Table 4.4: Localization Results and Error (Case 2)

Chapter 5 – Conclusion and Future work

In this thesis, PN codes are optimized for high-precision localization of multiple sources using pulsed UWB signals.

To get better localization results with pulsed UWB signals, the code design becomes critical issue. Gold codes have been employed in spread spectrum communications.

An algorithm to select an optimized subset of Gold codes is presented and a subset of 200 codes is chosen out of a set of 1025 Gold codes for localization analysis and experiments. The simulation begins with a setup for single source and demonstrates the way to find the exact source position. Subsequently we test the algorithm to detect 10 sources and calculate the position results.

To investigate the possibility of practical usage, an experiment has been carried out in a manufacturing building. Experimental devices such as Arbitrary Waveform Generator (AWG), Digital Serial Analyzer (DSA), and antennas for each experimental stage are introduced. The experiment is carried out for two different cases, one with 100 codes transmitted synchronously (Case 1) and one with random delays among the codes (Case 2). The localization results and errors of these two cases are presented.

In the thesis, all transmitters and receivers are set up in LOS conditions and one of two transmitters plays the role of interference due to limit of experimental devices. For practical usage of pulsed UWB localization, an experiment in Non-Line-of-Sight (NLOS) scenarios needs to be performed. In the current work, Gold codes are adopted for UWB localization. Better-optimized codes for UWB localization would further improve the performance.

Bibliography

[1] “First report and order 02-48,” Federal Communications commission, Feb. 2002.

[2] M. Ghavami, L. B. Michael, R. Kohno, Ultra Wideband signals and systems in communication engineering, Wiley, 2007.

[3] M. Z. Win and R. A. Scholtz, “Impulse radio: How it works,” *IEEE Commun. Lett.*, vol.2, no.2, pp. 36-38, 1998.

[4] H. Nikookar, R. Prasad, Introduction to Ultra Wideband for wireless communications, Springer, 2009.

[5] “U.S. Army Uses UWB to Track Trainees”, http://www.rfidjournal.com/article/articleview/1987/1/1/, accessed in August 2012.

[6] S. Gezici, Z. Tian, G. B. Giannakis, H. Kobayashi, A. F. Molisch, H. B. Poor, and Z., Sahinoglu, “Localization via ultra-wideband radios: A look at positioning aspects for future sensor networks,” IEEE *Signal Processing Mag.,* vol. 22, no.4, pp. 70-84, July 2005.

[7] H. Liu, H. Darabi, P.Ganerjee, and J. Liu, “Survey of wireless indoor positioning techniques and systems,” IEEE Systems, Man, and Cybernetics, vol. 37, no. 6, pp.1067-1080, Nov. 2007.

[8] Bernard Sklar, Digital Communications: Fundamentals and Applications, 2^{nd} ed., Prentice Hall, 2001.

[9] N. S. Correal, S Kyperountas, Q. Shi, and M. Welborn, “An UWB relative location system,” *IEEE Conf. Ultra Wideband Syst. Technol.,* pp. 394-397, Nov. 2003.

[10] Seungjin Baek, “Receiver synchronization for UWB TDOA localization,” Master Thesis, Oregon State University, US, 2010.

[11] Sarwate, D.V., and M.B. Pursley, "Crosscorrelation Properties of Pseudorandom and Related Sequences," *Proc. IEEE*, Vol. 68, No. 5, May, 1980, pp. 583-619.

[12] Gold, R. “Optimal binary sequences for spread spectrum multiplexing”. *IEEE Transactions on Information Theory*, October 1967, pp. 619-621.

[13] Proakis, John G., Digital Communications, Third edition, New York, McGraw Hill, 1995.

[14] Gold, R., "Maximal Recursive Sequences with 3-valued Recursive Cross-Correlation Functions," *IEEE Trans. Infor. Theory,* Jan., 1968, pp. 154-156.

[15] Ibe, Oliver C., Fundamentals of Applied Probability and Random Processes, Elsevier Inc., 2005.

[16] A. F. Molisch, K. Balakrishnan, D. Cassiloli, C. Chong, S. Emami, A. Fort, H. Karedal, J. Kunisch, H. Schantz, U. Schuster, K. Siwiak, "IEEE 802.15.4a channel model – final report", 2004.

[17] Y. Chan and K. Ho, "A Simple and Efficient Estimator for Hyperbolic Location," *IEEE Transactions on Signal Processing*, vol. 42, pp. 1905-1915, August 1994.

[18] D. Torrieri, "Statistical theory of passive location systems," *IEEE Trans. Aerosp. Electron. Syst.,* nol. 20, no. 2, pp. 183-197, Mar. 1984.